

Electrochemical corrosion of cast iron pipes in reclaimed water containing disinfectant

Haiya Zhang^{1,2}, Yimei Tian^{1,*}, Hao Guo¹, Mengxin Kang¹, Yarong Song¹

¹ School of Environmental Science and Engineering, Tianjin University, Tianjin 300350, China

² School of Environment, Tsinghua University, Beijing 100084, China

*E-mail: ymtian_2000@126.com

Received: 30 January 2018 / Accepted: 13 June 2018 / Published: 5 August 2018

The corrosion characteristics of cast iron pipes in reclaimed water containing 1, 2, and 4 mg/L NaClO and ClO₂ were investigated using potentiodynamic polarization curves (PPCs) and electrochemical impedance spectra (EISs). Scanning electron microscopy (SEM) was also used to evaluate the morphology of the corrosion scales. The results showed that NaClO and ClO₂ utilization changed the electron-transfer pathway and corrosion-product characteristics significantly. In reclaimed water containing NaClO at 1, 2, and 4 mg/L HClO could take precedence over dissolved oxygen (DO) to react with Fe and enhance the corrosion process at 4 days. However, the consumption of NaClO caused a shortage of HClO reacting with iron and induced the re-passivation of previously eroded areas at 30 days in the 1 mg/L NaClO experiments. Furthermore, high concentrations of NaClO (2 and 4 mg/L) also enhanced the corrosion process at 30 days. In the 1, 2, and 4 mg/L ClO₂ experiments, the ClO₂ molecule could take precedence over DO to react with the Fe and formed iron chlorides, enhancing the uniform corrosion throughout the whole experiment. Additionally, iron oxides or iron hydroxides usually showed a compact, needle-like structure in the control experiments, while flocculated iron chlorides were the main components in the disinfection experiments. Moreover, the acidification caused by H⁺ accumulation initiated distinct localized corrosion after 4 days of immersion in the 2 and 4 mg/L ClO₂ experiments, earlier than that in NaClO experiments (30 days). Thus, from a corrosion control perspective alone, NaClO is a better disinfection choice than ClO₂.

Keywords: disinfectant; electrochemical corrosion mechanism; cast iron; reclaimed water; corrosion scales;

1. INTRODUCTION

Reclaimed water distribution systems (RWDSs) usually work in the environment of a mixed electrolytic system including water, microorganisms, inorganic ions, and dissolved organic matter. Generally, the maintenance of a disinfectant residual is necessary to control bacterial growth.

Currently, many water professionals emphasize the important role of disinfectant residual on microorganism growth control [1], while less attention is focused on the corrosion effect. However, as strong oxidizers, disinfectants can interact with metal pipe materials directly, potentially inducing water-quality degradation and pipe corrosion [2-5].

Eisnor [6] investigated the effect of secondary disinfection on aged, unlined cast iron pipes by evaluating iron release and found that free chlorine increased the corrosion rate, while chlorine dioxide (ClO_2) had no effect on corrosion. Rahman [7] assessed the effect of secondary disinfectant (free chlorine, monochloramine, chlorine dioxide) on the corrosion process by measuring copper release and indicated that all disinfectants decreased copper release. However, in reality, iron corrosion is involved not only in electron loss from the metal base at the anode but also in chemical reduction at the cathode. Nevertheless, most research has evaluated the effect of disinfectant on metal corrosion based on measurements of metal release and weight loss, and little attention has been paid to the electrochemical corrosion properties.

However, the electrochemical corrosion-measurement approach is often used in harsh environments, particularly in high-ionic-content or acidic solutions [8]. Ha [9] studied the pit propagation kinetics in water containing a high concentration of anions by polarization curves (PCs) and electrochemical impedance spectra (EIS). Badea [10] investigated the corrosion and passivation behaviors in formic acid solutions using potentiostatic polarization curves (PPCs). Mandel [11] studied the electrochemical corrosion behavior of zirconia particle-reinforced high-alloy steel in sodium chloride solution using PPCs. Stoica [12, 13] also performed a number of electrochemical studies regarding stainless steel containing different biocidal and fungal suspensions.

In addition, Rios pointed out that metal corrosion behavior could not be analyzed in a straightforward manner in terms of the intrinsic reactivity of the metal but rather in terms of the characteristics of the metal corrosion film [14]. Considering the disinfectant, the crystalline characteristics, conductivity and porosity of the corrosion scale might also change the iron corrosion process [15, 16]. Montes [2] reported that NaClO considerably affects the copper corrosion mechanism and nature of corrosion products. EISs are usually used to analyze the electrical properties of corrosion scales in situ using frequency-specific information that enables the separation of the solution phase, corrosion scale, and charge-transfer resistance [17]. Alami [18] reported the effect of sulfate and dissolved oxygen on stainless-steel oxide films by EIS. González and Liu [19, 20] also analyzed the electrochemically reactive rust layer effect on metal corrosion resistance through EIS measurements. Nevertheless, the electron-transfer process in disinfected reclaimed water has not been well established.

Cast iron is a typical corrosion-resistant alloy, widely used in water and reclaimed-water distribution systems for its excellent ductility [21]. Thus, the focus of this project was to systematically evaluate the effect of reclaimed water containing 1, 2, and 4 mg/L NaClO and ClO_2 on the corrosion behavior of cast iron pipes using PPCs and EISs for a 30-day test. Furthermore, the corrosion film characteristics were investigated by scanning electron microscope (SEM). The localized corrosion characteristics were detected by advanced 3D digital microscope. These detailed methods might provide new insight into the methodology for understanding corrosion mechanisms in water

distribution systems. Finally, the analysis results should also provide a useful vision for the selection of a disinfectant strategy for corrosion control in water distribution systems.

2. MATERIALS AND METHODS

2.1 Materials and electrode preparation

The cast iron coupons used in the present study are composed of the following: C 19.08%, O 6.09%, Si 2.06%, Ca 0.58%, P 0.65%, S 1.60%, Fe 65%, Cu 1.98%, Mn 0.92%, and Zn 2.04%. The dissected cylindrical specimens with a 0.5 cm^2 working area were used as working electrodes; further, they were polished with a series of waterproof abrasive papers (200#, 400#, 600#, 800#, 1000#, 1200# and 1500#). Then, the working electrodes were connected with a copper wire and mounted with epoxy resin for the electrochemical test. Before use, the electrodes were degreased in acetone, dehydrated in absolute ethanol, dried in a laminar flow cabinet and exposed to ultraviolet light for 30 min.

2.2 Reclaimed water quality and disinfectant solution preparation

The reclaimed water was obtained from a reclaimed-water plant in northern China. The reclaimed water quality was kept stable throughout the entire experiment. The effluent water was sterilized in autoclaves at $120 \text{ }^\circ\text{C}$ for 20 min to eliminate the microorganism effect. Additionally, the oxygen was supplemented to maintain the initial DO concentration in effluent. The sterile water quality parameters are summarized in Table 1.

Table 1. Reclaimed water quality in present tests

Water quality parameter	Value	Water quality parameter	Value
pH	8.0 ± 0.5	Conductivity ($\mu\text{S}/\text{cm}$)	1555 ± 200
DO (mg/L)	7.5 ± 0.5	Cl^- (mg/L)	120.5 ± 20
Total bacteria count (CFU/mL)	0.0	SO_4^{2-} (mg/L)	221.0 ± 20
Total dissolved solids (mg/L)	713.0 ± 10.0	NO_3^- (mg/L)	14.2 ± 2.0

A commercially available chemically pure sodium hypochlorite (NaClO) stock solution (Jiangtian Chemical Corporation, China) was used to make chlorine solution. NaClO can release HOCl and OCl^- only when dissolved in water, and 1 mL NaClO solution has 0.117 mg active chlorine. Concentrated disinfectant solutions were produced in double-distilled water. The highly concentrated NaClO stock solution was diluted into the reclaimed water samples to reach the desired concentration of total chlorine (1, 2, or 4 mg/L). The total chlorine was measured by the DPD colorimetric method via a DR890 spectrophotometer (HACH Company, Loveland, Co, USA). Chlorine dioxide (ClO_2) was produced from chlorine dioxide powder (Hualong Xingyu Science and Technology Development Company, China). A 1 mg quantity of powder has 0.08 mg active chlorine dioxide; this powder was added into the reclaimed water samples to produce a certain concentration of chlorine dioxide (1, 2, or

4 mg/L). The target disinfectant values were chosen to be within minimum and maximum limits that have been established by regulatory agencies [22]. The pH and chlorine ion concentration in immersed reclaimed water were recorded at 1, 4, 12, 20 and 30 days according to a standard method (GB5749-2006). These values were measured to evaluate the corrosion process and the formation of secondary corrosion scales.

2.3 Electrochemical Immersion Test

To analyze the electron-transfer pathway in the corrosion process, conventional 250 mL three-electrode glass cells were used. Glass cells filled with reclaimed water without disinfectants were used as the control experiments, and the ones filled with reclaimed water containing known concentrations of NaClO or ClO₂ were used as experimental samples. The system was monitored by an electrochemical working station (KeSiTe, Wuhan Corrtest Instruments Corp., Ltd, China) for the 30-day experiments. All experiments were performed in triplicate and were carried out at room temperature (21.0±1.0 °C). A high-purity platinum (Pt) sheet and saturated Ag/AgCl were used as the counter electrode and reference electrode, respectively. No further oxygen supplementation measures were performed to simulate an actual reclaimed water distribution system, because sufficient DO was present in the front section, and later pipe sections were anoxic. Considering the transformations mediated by the corrosion reaction, electrochemical tests were performed at a representative 4 and 30 days. The disinfection supplementation period was 10 days to maintain the desired concentration. In addition, water quality parameters such as pH, DO, and chloride were measured according to standard methods [23].

Potentiodynamic polarization curve technology was introduced to obtain the anodic and cathodic electron-transfer process under the disinfection effect. PPCs were obtained with a scanning rate of 0.5 mV/s over a range of -0.1 V to 0.1 V around the open-circuit potential. EIS was carried out to evaluate the corrosion-product film formation, adsorption and diffusion processes. EIS over a frequency range of 100 000 Hz to 0.01 Hz and with a sinusoidal signal amplitude of 10 mV was conducted for different immersion periods. Before PPC and EIS tests, the open-circuit potential was tested for 20 min for system stability. Finally, the EIS data were analyzed with ZSimpWin software and fitted with corresponding equivalent electric-circuit models.

2.4 Corrosion scales and localized corrosion characterization

Electroactive corrosion scales play a significant role throughout the corrosion process. After immersion tests, the morphology and elemental composition of corrosion scales were examined by S4800 field emission scanning electron microscopy (Hitachi Company, Japan). After removing the corrosion products, the coupons were cleaned with a mixed fluid of hydrochloric acid and hexamethylenetetramine, soaked in ethyl alcohol and dried with filter paper. Finally, the localized corrosion characteristics of the coupons were detected by an advanced 3D digital microscope (Hirox KH-7700, Hirox CO., Ltd, Japan). In the testing process, the maximum corrosive pitting was found

when performing an overall scan on the electrode surface. Then, this pit depth was measured based on the un-corroded areas.

3. RESULTS AND DISCUSSION

3.1 Variations of water quality

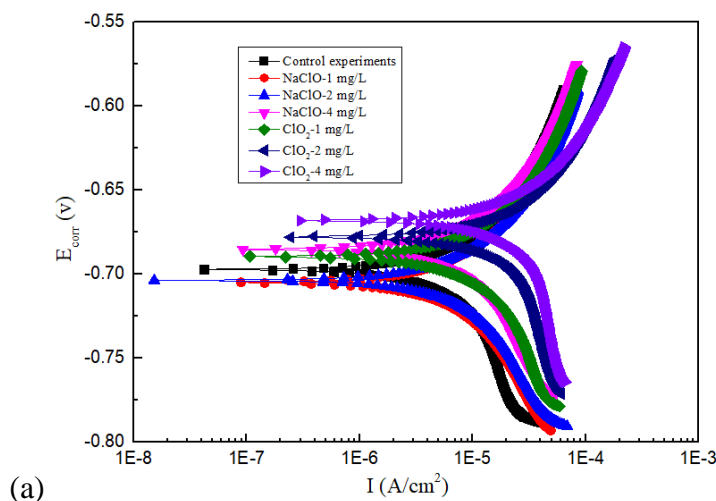
Table 2. The pH values and chloride ion contents in control, NaClO and ClO₂ experiments

Parameter	Control experiments	NaClO experiments			ClO ₂ experiments		
		1 mg/L	2 mg/L	4 mg/L	1 mg/L	2 mg/L	4 mg/L
pH	8.0±0.5	8.1±0.3	8.3±0.2	8.4±0.3	7.81±0.3	7.63±0.4	7.56±0.5
Cl ⁻ (mg/L)	120.5±20	125.6±12	132.8±10	143.6±8	122.8±11	125.6±8	126.4±9

The pH values and chloride ion contents in the control, NaClO and ClO₂ experiments are shown in Table 2, because the chemical properties of NaClO and ClO₂ are highly dependent on pH values. In control tests, the pH values remained stable at 8.0±0.5. In NaClO experiments, the pH values increased gradually due to the hydrolysis reaction of NaClO, which also increased with the disinfectant concentration. In contrast, the pH values in ClO₂ experiments decreased gradually due to the reaction between ClO₂ and Fe²⁺, which will be discussed in the electrochemical corrosion section.

The trend of chloride (Cl⁻) concentration was also considered because this species might be involved in the localized corrosion and corrosion-scale formation processes. The Cl⁻ concentration was 120.5±20 mg/L in the initial reclaimed water. Upon NaClO utilization, the Cl⁻ concentration increased sharply, reaching a maximum value of approximately 143.6±8 mg/L in the 4 mg/L NaClO experiments. However, upon ClO₂ addition, the Cl⁻ concentration presented slightly higher values than those in the controls.

3.2 Potentiodynamic polarization curve (PPC) results



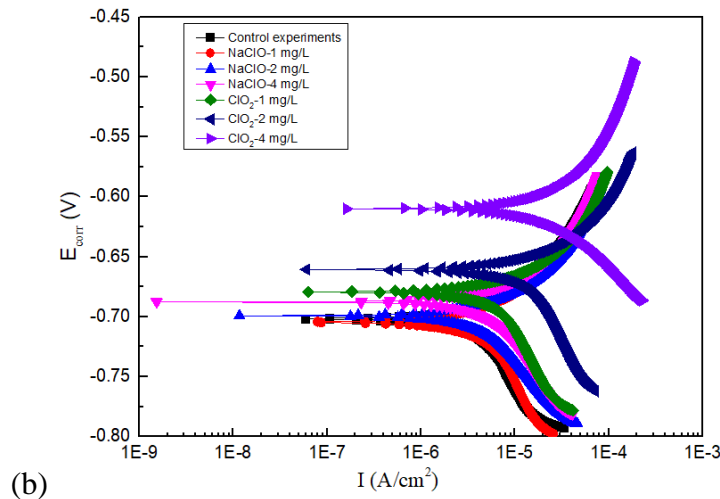


Figure 1. The potentiodynamic polarization curves of cast iron pipes in controls and reclaimed water containing 1, 2, and 4 mg/L NaClO and ClO₂ at (a): 4 days; (b): 30 days

The potentiodynamic polarization curves of cast iron pipes in controls and reclaimed water containing 1, 2, and 4 mg/L NaClO and ClO₂ can be seen in Fig 1(a) (4 days) and 1(b) (30 days). The fitting results of these polarization curves, including the anodic and cathodic Tafel slopes (β_a , β_c), corrosion potential (E_{corr}), and corrosion current density (I_o), can be seen in Table 3 (4 days) and Table 4 (30 days).

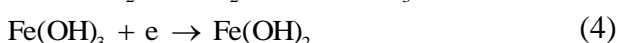
Table 3. The fitting results of polarization curves in control, NaClO and ClO₂ experiments at 4 days

Experiment category	β_a (mV/decade)	β_c (mV/decade)	I_o (A/cm ²)	E_o (V)
Control experiments	87	125	5.625×10^{-6}	-0.697
NaClO-1 mg/L	78	81	5.725×10^{-6}	-0.704
NaClO-2 mg/L	68	75	1.409×10^{-5}	-0.705
NaClO-4 mg/L	94	99	4.315×10^{-6}	-0.688
ClO ₂ -1 mg/L	88	121	4.830×10^{-6}	-0.679
ClO ₂ -2 mg/L	98	108	1.019×10^{-5}	-0.661
ClO ₂ -4 mg/L	102	69	1.901×10^{-5}	-0.609

Table 4. The fitting results of polarization curves in control, NaClO and ClO₂ experiments at 30 days

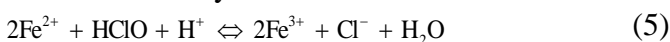
Experiment category	β_a (mV/decade)	β_c (mV/decade)	I_o (A/cm ²)	E_o (V)
Control experiments	57	240	2.578×10^{-5}	-0.702
NaClO-1 mg/L	62	244	2.514×10^{-5}	-0.704
NaClO-2 mg/L	45	130	3.500×10^{-5}	-0.699
NaClO-4 mg/L	46	163	3.837×10^{-5}	-0.687
ClO ₂ -1 mg/L	41	221	5.115×10^{-5}	-0.679
ClO ₂ -2 mg/L	43	126	8.933×10^{-5}	-0.660
ClO ₂ -4 mg/L	108	85	14.24×10^{-5}	-0.609

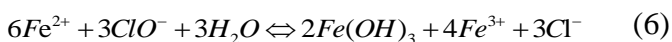
According to the data from control experiments, E_{corr} was relatively negative at 4 days. In the initial stage of experiments, the dissolved oxygen (DO) was sufficient in the reclaimed water (7.5 mg/L). As the only cathode depolarizer, DO could accept the electrons coming from anodic iron dissolution and was reduced to OH^- (Eq.1; Eq.2), revealing the activation effect of oxygen on iron (Eq.3). During this experiment, DO values declined gradually in the closed reclaimed water system (S1). As the DO concentration decreased, the corrosion process decreased sharply because iron oxides are thermodynamically stable. The higher β_c values at 30 days also confirmed this large reaction resistance, which might be caused by the lower electronic capacity of the corrosion scale. Meanwhile, the E_{corr} values also actually shifted to positive values during the period of 4 days to 30 days. However, the corrosion current density (I_o) increased sharply, and β_c became far greater than β_a , demonstrating that a localized corrosion reaction might have occurred and that the cathodic reaction became the corrosion control step. We assumed that in the dissolved-oxygen-deficient environment, the preformed $\text{Fe}(\text{OH})_3$ could also serve as the oxidant to accept electrons and be reduced to $\text{Fe}(\text{OH})_2$ (Eq.4), enhancing the localized corrosion reaction [24]. Simultaneously, the localized corrosion reaction was noticeably accelerated, due to the corrosion-scale transformation process and the obviously uneven distribution of DO concentrations [25].



As indicated in Fig 1 and Table 3, the corrosion current density (I_o) in reclaimed water containing 1, 2, or 4 mg/L NaClO or ClO_2 was higher than that in the control experiments at 4 days, demonstrating that utilization of two disinfectants enhanced the corrosion process. Additionally, it was found that the cathodic Tafel slopes (β_c) in all disinfected experiments were lower than those in control experiments.

In NaClO experiments, considering the disinfectant-residual decay, intermittent dosing of sodium hypochlorite was needed to maintain the disinfectant concentration and reestablish reaction equilibrium, leading to a continuous increase in Cl^- . Sodium hypochlorite might also undergo different chemical reactions with varying pH values in the water phase. From the pH trend, HClO and ClO^- were both present at the pH values used in the present experiments [3]. Therefore, HClO or ClO^- might be the predominant component, reacting preferentially with the Fe^{2+} rather than DO and resulting in the gradually decreased cathodic Tafel slope (β_c) at 4 days. In other words, HOCl or ClO^- likely participated in the cathodic depolarization process, enhancing the electron transfer efficiency and changing the oxygen-activated corrosion mechanism in control tests (Eq.5; Eq.6). During this process, the positively charged Fe^{2+} was consumed quickly, and $\text{Fe}(\text{OH})_3$ was formed at the anode accordingly (Eq.7). At the same time, the accumulated Cl^- on the electrode surface contributed to the negative shift in E_{corr} . In addition, excess Cl^- could react with the corrosion products and change their morphology (Eq.8; Eq.9). Taken together, the corrosion current density (I_o) in reclaimed water containing NaClO presented higher values than that in the control experiments at 4 days, demonstrating that the corrosion process was enhanced by NaClO .





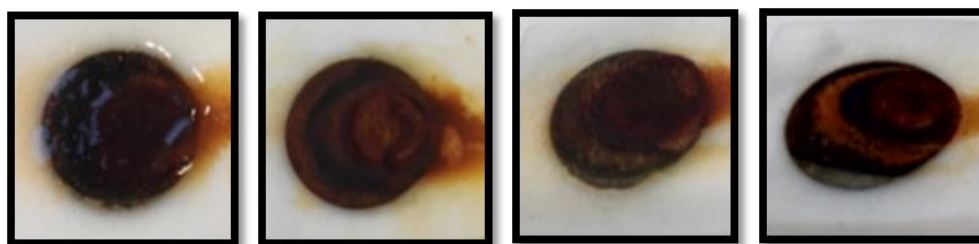
However, the reaction between the HClO and Fe^{2+} also led to increased pH values. Moreover, this highly alkaline environment might also have facilitated the transformation of preformed $\text{Fe}(\text{OH})_3$ to Fe_3O_4 [26], improving the corrosion product stability. Therefore, this corrosion scale became an obstacle to the electron transfer process and accelerated the disinfectant consumption. Given this reason, a shorter period with a lower disinfectant residual might change the corrosion mechanism in the 1 mg/L NaClO experiments. Even if there is chloride attacking a metal surface, the pitting area could be re-passivated quickly by hydroxide ions, presenting a short retarding period. Consequently, the cathodic Tafel slope (β_c) and E_{corr} increased sharply in the 1 mg/L NaClO experiments and presented higher values than that in the control. These results verified that reclaimed water containing 1 mg/L NaClO retarded the corrosion process indirectly at 30 days, leading to a reduction in corrosion current density (I_0). However, in the 2 and 4 mg/L NaClO experiments, the abundant HClO or ClO^- could always act as an additional depolarizer and reacted preferentially with Fe^{2+} , and enhanced the corrosion process at 30 days.

In ClO_2 tests, the cathodic Tafel slope (β_c) dropped sharply compared with those in both NaClO and control experiments, resulting in a direct amplification of the corrosion current density (I_0). Thus, there are good reasons to believe that the indecomposable ClO_2 molecules as a whole were the active cathodic depolarizing species and accepted the electrons firsthand rather than DO (Eq.10). Meanwhile, lower pH values also caused the H^+ to be in a more active state, inducing hydrogen evolutionary corrosion (Eq.11).



However, an interesting phenomenon was that E_{corr} showed a distinct ennoblement in the ClO_2 experiments, demonstrating that the accelerated electron-transfer process did not cause the drop in E_{corr} . It is likely that electrical currents caused by the chemical reactions passed through the liquid medium quickly, without pausing on the metal surface. In short, from the obtained electrochemical parameters, it was clearly observed that the reclaimed water with ClO_2 exhibited a higher corrosion rate compared with those in both NaClO and control experiments.

3.3 Structure and composition of the corrosion scales



(a) Control (b) NaClO-1 mg/L (c) NaClO-2 mg/L (d) NaClO-4 mg/L

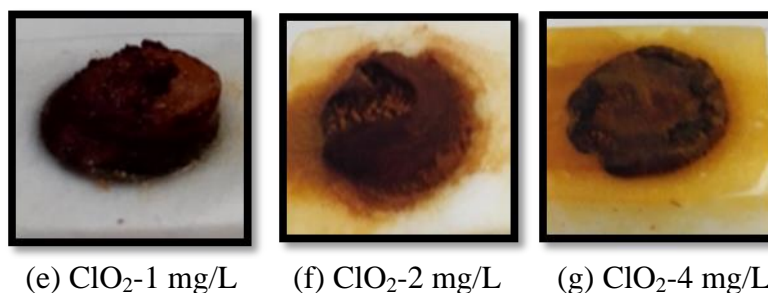


Figure 2. Corrosion scales characteristic of the cast iron surface at 30 days

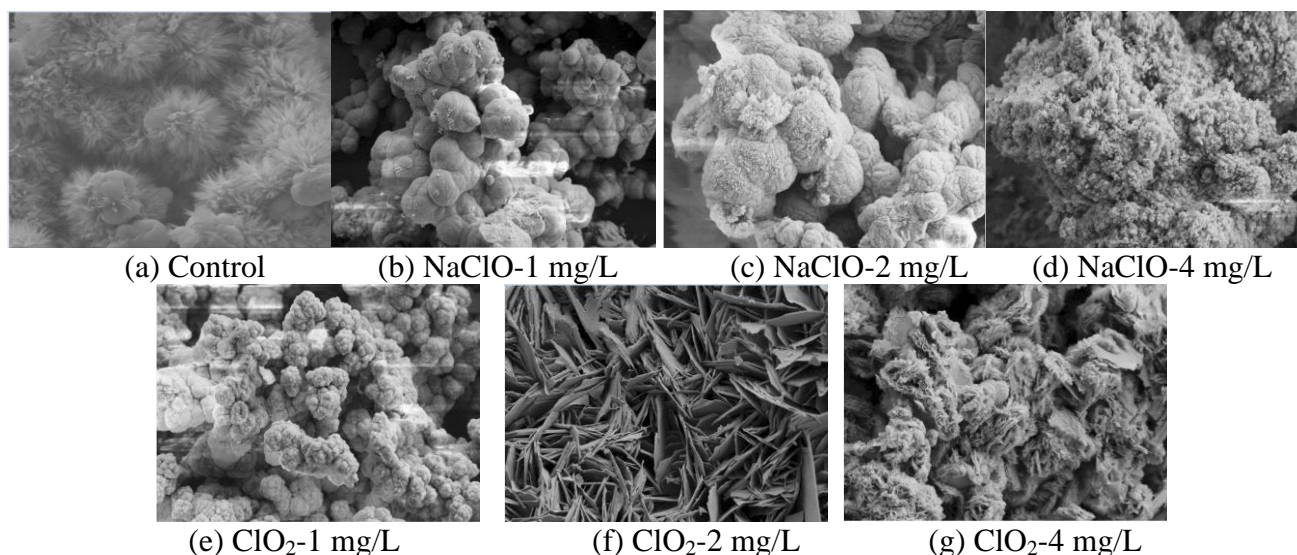
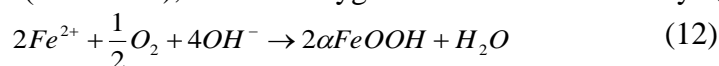


Figure 3. SEM results of corrosion scales on the cast iron surface at 30 days

When the cast iron pipes were immersed into the disinfectant-containing reclaimed water, the physicochemical characteristics of the corrosion scales on the pipe surface might also be modified. Fig 2 and Fig 3 show the corrosion scales and SEM results ($\times 5000$) on the cast iron surface in (a) control; (b) 1 mg/L NaClO; (c) 2 mg/L NaClO; (d) 4 mg/L NaClO; (e) 1 mg/L ClO₂; (f) 2 mg/L ClO₂; and (g) 4 mg/L ClO₂ experiments after 30 days. From visual inspection, the corrosion scales were similar for samples in all experiments, and all scales were composed of black and dark-brown materials. However, the density, thickness and uniformity appeared to be different.

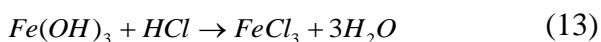
The corrosion scales in the control experiments were more substantial but incomplete, with a black base on the metal surface. Combined with the PPC results, it can be inferred that the scales closest to the scale-water interface were in the ferric iron state due to the relatively high DO values, while the region closest to the metal-scale surface had more of the ferrous phase. In addition to Fe(OH)₃ and Fe(OH)₂, the corrosion scales presented a needle-like structure, which were identified as goethite (α -FeOOH), in a low-oxygen environment at 30 days (Eq.12) [27].



When immersed into reclaimed water containing NaClO, HClO or ClO⁻ can react with Fe²⁺ preferentially rather than dissolved oxygen (Eq.5; Eq.6). Meanwhile, the highly concentrated chloride

ions can also be adsorbed on the metal surface [28], leading to the dissolution of the passive film after reaction (Eq.6; Eq.7). The higher floc content in Fig 3(c) and Fig 3(d) also confirmed this phenomenon. However, round-shaped corrosion products identified as Fe_3O_4 appeared in Fig 3(b), confirming that instantaneous passivation occurred in the 1 mg/L $NaClO$ experiments at 30 days.

In ClO_2 -containing reclaimed water, the scales exhibited a structure with very few granular crystals interspersed on a floc-like matrix, and no obvious crystalline phase was found, which demonstrated that the preformed $Fe(OH)_3$ might be dissolved (Eq.13) at relatively lower pH values. The increasing I_0 values also explained the solubility and poor protective properties of these corrosion scales. Thus, it is important to point out that ClO_2 limited the formation of a compact crystalline phase, leading to much looser corrosion scales.



3.4 Localized corrosion analysis

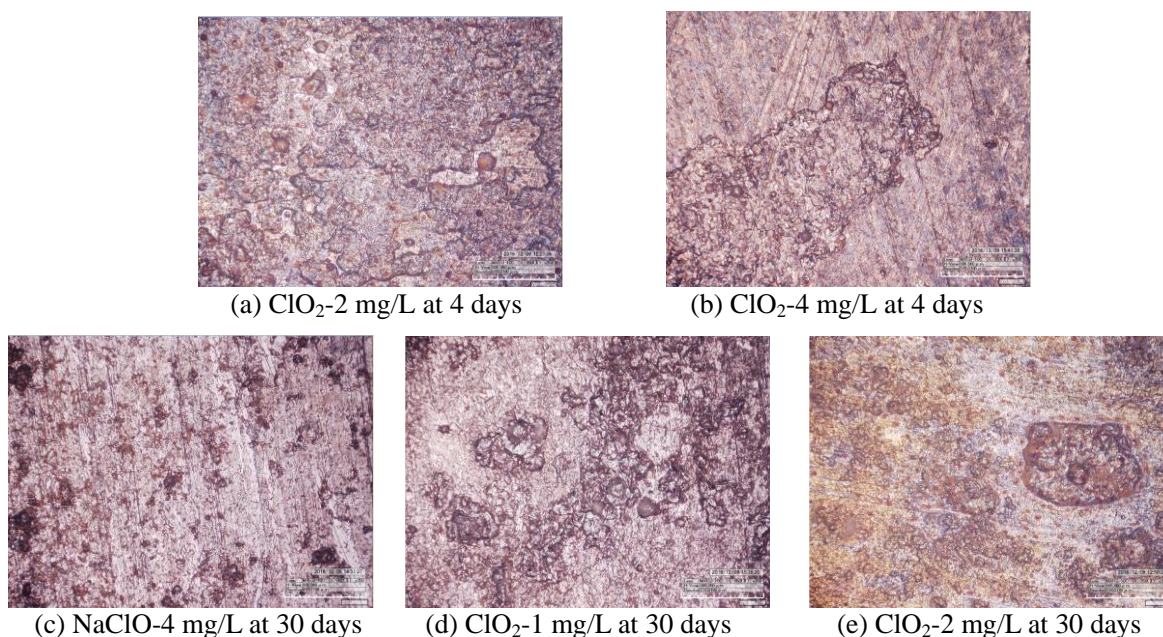


Figure 4. Localized corrosion results of cast iron pipes in (a) ClO_2 -2 mg/L at 4 days; (b) ClO_2 -4 mg/L at 4 days; (c) $NaClO$ -4 mg/L at 30 days; (d) ClO_2 -1 mg/L at 30 days; (e) ClO_2 -2 mg/L at 30 days

Localized corrosion is one of the most important forms of corrosion and is more dangerous than uniform corrosion because it is more difficult to predict and counteract [29]. In particular, only a small pit with minimal metal loss might lead to the failure of the whole pipe [30]. The localized corrosion results were analyzed as shown in Fig 4.

Localized corrosion was a comprehensive and long-term effect. In the 2 and 4 mg/L ClO_2 experiments, wide-ranging localized corrosion could be seen at 4 days. This largest localized corrosion was probably attributed to the high anodic dissolution rate at lower pH, which might also be related to

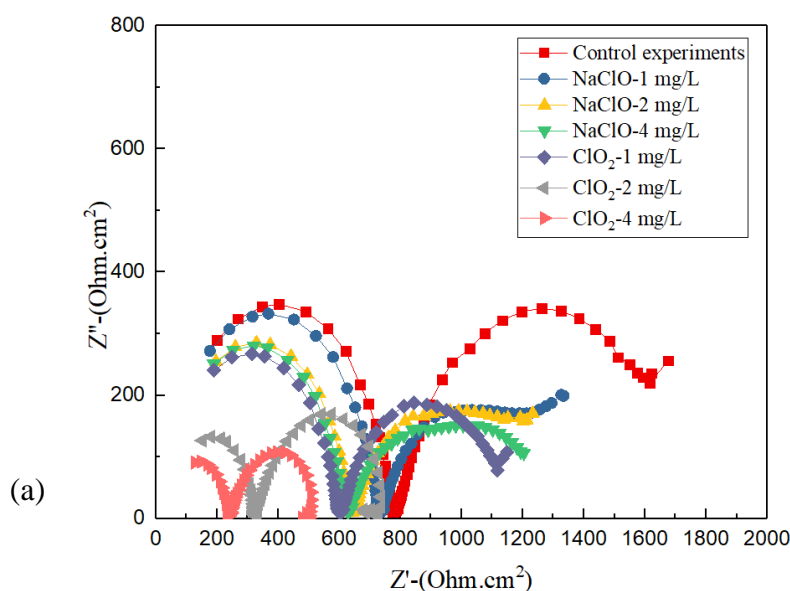
the transformation of iron oxides to iron chlorides (Eq.13). The largest corrosion pit width and depth were 175.557 μm and 11.207 μm in the 2 mg/L ClO_2 experiments, respectively, and these parameters were 19.239 μm and 26.117 μm in the 4 mg/L ClO_2 experiments, respectively.

In contrast, in NaClO experiments, only cast iron in reclaimed water with 4 mg/L NaClO presented localized corrosion after 30 days. The largest corrosion pit width and depth were 211.041 μm and 21.506 μm , respectively. This result might suggest that a relatively high chloride content can combine with the corrosion products, penetrate through the porous corrosion film and induce localized corrosion at 30 days in NaClO experiments. However, the corrosion scope and corrosion pit depth were all smaller than those in ClO_2 experiments, even those observed in the 1 mg/L ClO_2 experiments. Additionally, the localized corrosion scope of 2 mg/L ClO_2 continued to expand at 30 days.

Thus, in summary, the relatively higher H^+ activity in the 2 and 4 mg/L ClO_2 experiments induced localized corrosion at 4 days. In NaClO experiments, the relatively higher pH values delayed the occurrence of localized corrosion, making the localized corrosion incubation period (30 days) significantly longer than that observed for ClO_2 (4 days) and the corrosion width and corrosion pit depth much smaller than those previously observed.

3.6 EIS results

Nyquist plots of the cast iron electrode in the control, NaClO and ClO_2 experiments are shown in Fig 5(a) (4 days) and Fig 5(b) (30 days). In Fig 5(a), all the impedance spectra recorded were composed of two capacitive semicircles. The first capacitive semicircle at high frequency was probably related to the corrosion-scale resistance, and the second capacitive semicircle at low frequency was related to the electron-transfer resistance [31.32]. From Fig 5(a), it can be found that the capacitive spectra at high frequency and low frequency were higher in control experiments than in reclaimed water samples containing disinfectant, suggesting the enhancing effect of disinfection on the corrosion process. Moreover, the capacitive spectra at low frequency had a curved end in the reclaimed water containing 2 and 4 mg/L ClO_2 , confirming the occurrence of localized corrosion.



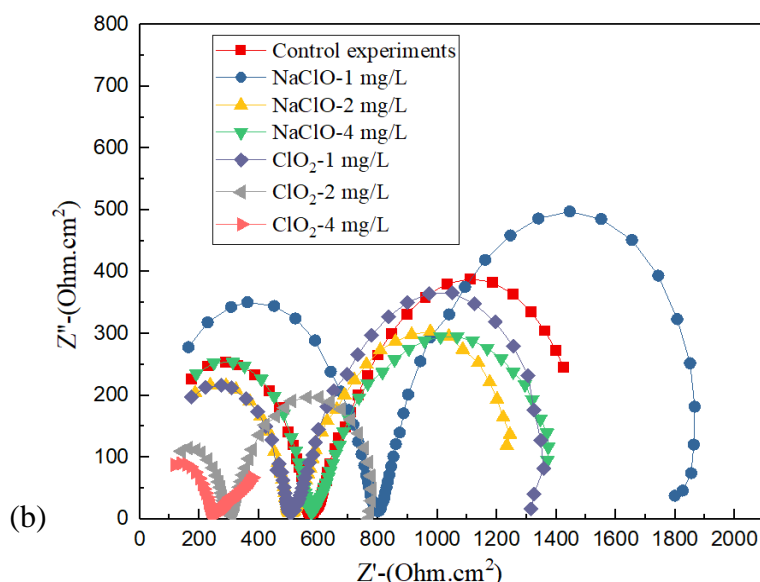


Figure 5. Nyquist plots of cast iron electrode in control, NaClO and ClO₂ experiments at (a): 4 days; (b): 30 days

For better EIS comparative analysis, the impedance spectra recorded for each immersion time were fitted with an equivalent circuit with two time constants, illustrated as $R_s(CPE1(R_f(CPE2R_{ct})))$. The fitted results of Nyquist plots for the control, NaClO and ClO₂ experiments at 4 days are shown in Table 5. Constant phase elements (CPEs) were used to replace the capacitors in equivalent circuits due to surface inhomogeneity.

Table 5. Fitted results of Nyquist plots for the control, NaClO and ClO₂ experiments at 4 days

Experiment category	R_s ($\Omega.cm^2$)	R_f ($\Omega.cm^2$)	$CPE1$ ($\mu F.cm^{-2}$)	n_f	R_p ($\Omega.cm^2$)	$CPE2$ ($\mu F.cm^{-2}$)	n_{dl}
Control experiments	24.34	749.5	7.384 E-9	0.950	1008	0.00128	0.738
NaClO-1 mg/L	22.05	699.8	6.618 E-9	0.965	778.7	0.00171	0.572
NaClO-2 mg/L	26.29	605.9	6.801 E-9	0.961	730.6	0.00168	0.591
NaClO-4 mg/L	20.85	596.1	6.997 E-9	0.960	692.4	0.00146	0.550
ClO ₂ -1 mg/L	19.54	577.5	8.625 E-9	0.948	576.6	0.00108	0.716
ClO ₂ -2 mg/L	17.61	299.6	1.884 E-8	0.916	405.4	0.00077	0.855
ClO ₂ -4 mg/L	10.72	218.8	2.793 E-8	0.896	272.1	0.00085	0.829

In Table 5, R_s represents the solution resistance, R_f is the corrosion-scale resistance and R_{ct} is the charge-transfer resistance. CPE1 is associated with the capacitance of the corrosion scale, and CPE2 is the constant phase element related to the metal-electrolyte double layer. Here, resistances and capacitances are either related to the corrosion products formed on the iron surface or the redox processes occurring in the metal layer. In control experiments, the values of corrosion-scale resistance R_f were always lower than the charge-transfer resistance R_{ct} values, implying that the electron transfer process was the corrosion control step.

When compared with the control, the R_{ct} and R_f values in reclaimed water containing NaClO or ClO_2 were all smaller at 4 days, showing that HOCl or ClO_2 enhanced the electron-transfer process, changed the electron-transfer pathway and reduced the compactness of corrosion scales. As mentioned before, the corrosion scales formed on the iron surface seemed to be mainly composed of $Fe(OH)_3$ in control experiments. The lower R_f values and higher CPE1 values in NaClO experiments indicated that the chlorides could gradually replace the hydroxide in the corrosion products (Eq.8; Eq.9). Meanwhile, the chloride content inside the scales had high electronic conductivity and facilitated the movement of electrons outward from the metal-scale interface. In contrast, the lower R_f values and higher CPE1 values in ClO_2 experiments demonstrated that relatively lower pH values led to the dissolution of the preformed $Fe(OH)_3$ (Eq.13).

In Fig 5(b), the recorded impedance spectra were also composed of two capacitive semicircles, except for that in reclaimed water containing 4 mg/L ClO_2 . The impedance spectra were also fitted using the equivalent circuit with two time constants, illustrated as $R_s (CPE1(R_f(CPE2R_{ct})))$. The fitted results can be seen in Table 6. The impedance spectra in reclaimed water containing 4 mg/L ClO_2 were simulated using the equivalent circuit with the Warburg diffusion impedance, identified as $R_s (CPE_f(R_f(W)))$. The fitted results can be seen in Table 7.

Table 6. Fitted results of Nyquist plots for control, NaClO and ClO_2 experiments at 30 days, except for the 4 mg/L ClO_2 experiments

Experiment category	R_s ($\Omega.cm^2$)	R_f ($\Omega.cm^2$)	$CPE1$ ($\mu F.cm^{-2}$)	n_f	R_p ($\Omega.cm^2$)	$CPE2$ ($\mu F.cm^{-2}$)	n_{dl}
Control experiments	17.6	625.4	9.066 E-9	0.937	1336	0.00199	0.783
NaClO-1 mg/L	42.46	797.4	1.145 E-8	0.920	1132	0.00106	0.875
NaClO-2 mg/L	27.17	503.3	1.500 E-8	0.902	868.2	0.00204	0.734
NaClO-4 mg/L	15.13	549.3	7.953 E-9	0.950	883	0.00137	0.716
ClO_2 -1 mg/L	28.0	465.5	9.589 E-9	0.950	907.7	0.00150	0.821
ClO_2 -2 mg/L	25.7	302.8	2.618 E-8	0.899	511.1	0.00185	0.812

Table 7. Fitted results of Nyquist plots for the 4 mg/L ClO_2 experiment at 30 days

Experiment category	R_s ($\Omega.cm^2$)	R_f ($\Omega.cm^2$)	$CPE1$ ($\mu F.cm^{-2}$)	n_f	$WI-R$ ($\Omega.cm^2$)	$WI-T$ ($\mu F.cm^{-2}$)	$WI-P$
ClO_2 -4 mg/L	17.6	226	5.293 E-8	0.85	808.5	9250	0.255

From Table 6, the R_f value for the control experiment presented a decreasing trend, probably indicating the disruption of the outer corrosion scales in the closed environment. This may have occurred because the preformed $Fe(OH)_3$ or α - $FeOOH$ could be used as the new cathode, resulting in the reduction of corrosion products and the consumption of electrons, and also enhance the corrosion process indirectly.

In reclaimed water containing 1 mg/L NaClO, the impedance spectra increased sharply at 30 days, showing constantly growing resistance to the corrosion reaction. It can be speculated that the lower radius of OH⁻ might have penetrated the corrosion products easily and enabled the re-passivation of the pre-eroded areas in the reclaimed water without sufficient disinfection at 30 days. Thus, the cast iron surface is prone to the formation of a passivation layer that shifts the double layer and charge-transfer resistance from the water/scale interface to the corrosion scale/metal interface at the sampled times in reclaimed water containing 1 mg/L NaClO. However, as the disinfection concentration increased, adequate HClO or ClO⁻ molecules could promote the corrosion process to the same degree as that observed at 4 days. This promotion phenomenon in ClO₂ experiments at 30 days was the same as that in the 4-day tests.

Based on EIS analysis, the corrosion behavior seems to be strongly dependent on the film structure. It is worth stressing that variation in CPE1 is related to changes in the corrosion products. The trend of variation in CPE1 values in control experiments demonstrated the formation of a corrosion passivation layer at 4 days and the rupture of the complete corrosion layer at 30 days. When considering disinfectant addition, the higher CPE1 values in ClO₂ experiments confirmed the greater thickness or higher electreactivity of the corrosion scales in the disinfection process [19].

5. CONCLUSION

The electrochemical corrosion behavior of cast iron pipes in disinfectant-containing reclaimed water was investigated using potentiodynamic polarization curves (PPCs) and electrochemical impedance spectra (EISs). The results showed that NaClO and ClO₂ utilization changed the electron-transfer pathway and corrosion-product characteristics significantly. In control experiments, the sufficient DO concentration activated the dissolution of Fe at the anode after 4 days immersion. As the corrosion reaction proceeded, the reclaimed water experienced a status transition from aerobic status to anoxic status, enabling the preformed corrosion product Fe(OH)₃ to be used as the new cathode and promoting further anodic iron dissolution at 30 days. In reclaimed water containing 1, 2, or 4 mg/L NaClO, HClO or ClO⁻, this procedure could take precedence over the dissolved oxygen (DO) response with Fe and enhance the corrosion process at 4 days. However, the consumption of NaClO caused a shortage of HClO reacting with iron, and induced the re-passivation of previously eroded areas at 30 days in 1 mg/L NaClO experiments. Furthermore, high concentrations of NaClO (2 and 4 mg/L) also enhanced the corrosion process at 30 days. In 1, 2, and 4 mg/L ClO₂ experiments, the ClO₂ molecule could take precedence over DO to react with the Fe and formed iron chlorides, enhancing the uniform corrosion throughout the whole experiment. Additionally, iron oxides or iron hydroxides usually showed compact, needle-like structures in control experiments, while flocculated iron chlorides were the main components in disinfection experiments. Moreover, the acidification caused by H⁺ accumulation initiated distinct localized corrosion after 4 days of immersion in the 2 and 4 mg/L ClO₂ experiments, which was earlier than that in NaClO experiments (30 days). Thus, from a corrosion control perspective alone, NaClO is a better disinfection choice than ClO₂.

FUNDING

This work was supported by National Natural Science Foundation of China (No. 51478307) and the Specialized Research Fund for the Doctoral Program of Higher Education of China (No. 20130032110032)

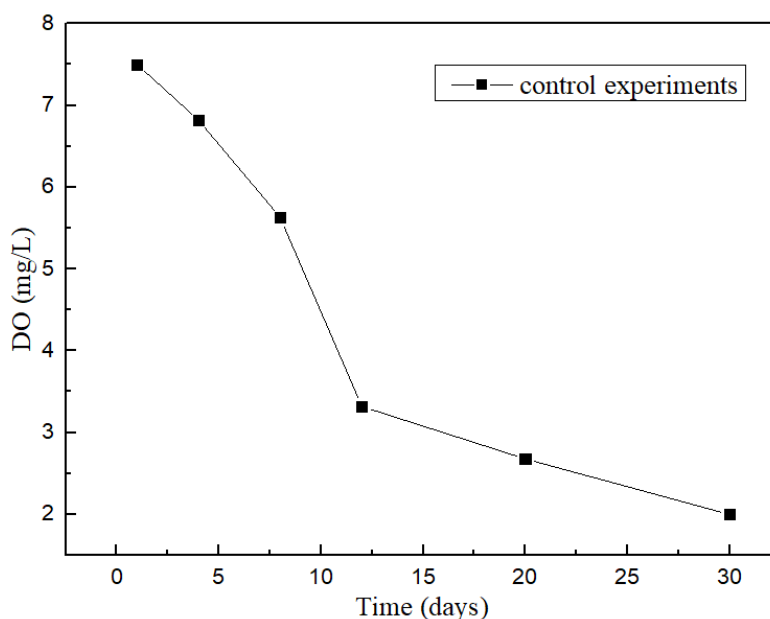


Figure S1. The DO values of reclaimed water in control experiments

References

1. A. Allue-Guardia, A. Martinez-Castillo, M. Muniesa, *Appl. Environ. Microb.*, 80 (2014) 2142.
2. J. C. Montes, F. Hamdani, J. Creus, S. Touzain, O. Correc, *Appl. Surf. Sci.*, 314 (2014) 686.
3. A. F. Cantor, J. K. Park, P. Vaiyavatjamai, *J. Am. Water Works Ass.*, 5 (2003) 112.
4. A. E. Broo, B. Berghult, T. Hedberg, *Water Sci Tech-W Sup.*, 1 (2001) 117.
5. M. Moore, *Am. J. Clin. Nutr.*, 89 (2001) 838.
6. J. D. Eisnor, G.A. Gagnon, *J. Water Supply Res. T.*, 53 (2004) 441.
7. S. Rahman, B. C. McDonald, G. A. Gagnon, *J Environ Eng.*, 133 (2007) 180.
8. Z. B. Wang, H. X. Hu, Y. G. Zheng, *J. Solid State Electr.*, 20 (2016) 3459.
9. H. Ha, C. Taxen, K. Williams, J. Scully, *Electrochim. Acta.*, 56 (2011) 6165.
10. G. E. Badea, D. Ionita, P. Cret, *Mater Corros.*, 65 (2014) 1103.
11. M. Mandel, L. Krüger, S. Decker, *Mater Corros.*, 66 (2015) 1456.
12. M. Stoica, M. Bruma, G. Carac, *Mater. Corros.*, 61 (2010) 1017.
13. M. Stoica, L. Mikoliunaite, A. Ramanaviciene, P. Alexe, G. Carac, R. Dinica, J. Voronovic, A. Ramanavicius, *Chemija.*, 23 (2012) 180.
14. J. F. Rios, J. A. Calderon, R. P. Nogueira, *Corrosion -Houston Tx.*, 69 (2013) 875.
15. D. A. Lytle, J. Liggett, *Water Res.*, 92 (2016) 11.
16. T. L. Gerke, J. B. Maynard, M. R. Schock, D. L. Lytle, *Corros. Sci.*, 50 (2008) 2030.
17. V. F. Lvovich, *Electrochemical Impedance Spectroscopy-Theory and Applications [M]*. 2012.
18. A. Alami, M. Bojinov, *J. Solid State Electr.* (2017)., doi: 10.1007/s10008-017-3691-3.
19. J. A. Gonzalez, J. M. Miranda, E. Otero, S. Feliu, *Corros. Sci.*, 49 (2007) 436.
20. M. Liu, X. Cheng, G. Zhao, X. Li, Y. Pan, *Surf. Interface Anal.*, 48 (2016) 981.
21. Y. Wang, X. Zhang, Y. Chen, P. Lu, C. Chen, *Environmental Science.*, 30 (2009) 3293.

22. GB/T 18920-2002, Reuse of recycling water for urban water quality standards for urban miscellaneous water consumption. China, Beijing, 2002.
23. GB/T 5750.1-2006, Standards for drinking water quality, China, Beijing, 2006.
24. H. Guo, Y. Tian, H. Shen, X. Liu, Y. Chen, *Int J. Electrochem Sci.*, 11 (2016) 6993.
25. G. D. Eyu, G. Will, W. Dekkers, J. MacLeod, *Materials (Basel, Switzerland)*., 9 (2016) 748.
26. R. M. Cornell, U. Schwertmann, *Corro. Sci.*, 39 (1997) 1499.
27. B. J. Little, J. S. Lee, T. L. Gerke, *Corrosion -Houston Tx-*., 73 (2017) 138.
28. P. Q. Zhang, J. X. Wu, W. Q. Zhang, X. Y. Lu, K. Wang, *Corros. Sci.*, 34 (1993) 1343.
29. M. Mehanna, R. Basseguy, M. Delia, A. Bergel, *Corros. Sci.*, 51 (2009) 2596.
30. . Suzuki, Y. Ishikawa, Y. Hisamatsu, *Corros. Sci.*, 23 (1983):1095.
31. D. C. Kong, C. F. Dong, X. Q. Ni, A.N. Xu, C. He, K. Xiao, X.G. Li, *Mater. Corros.*, 68 (2017) 1070.
32. J. J. Shim, J. G. Kim, *Mater. Lett.*, 58 (2004) 2002.

© 2018 The Authors. Published by ESG (www.electrochemsci.org). This article is an open access article distributed under the terms and conditions of the Creative Commons Attribution license (<http://creativecommons.org/licenses/by/4.0/>).